

Entrapment of rhodium complexes in inorganic or hybrid matrices *via* the sol–gel method

José Daniel Ribeiro de Campos and Regina Buffon*

Instituto de Química, Universidade Estadual de Campinas, P.O. Box 6154, 13083-970, Campinas-SP, Brazil. E-mail: rbuffon@iqm.unicamp.br; Fax: +55 19 3788 3023; Tel: +55 19 3788 3090

Received (in Montpellier, France) 31st July 2002, Accepted 7th October 2002

First published as an Advance Article on the web 2nd January 2003

Rhodium complexes have been entrapped inside the porous systems of inorganic or hybrid matrices *via* the sol–gel method. The resulting materials were tested as catalysts in hydroformylation reactions. The microporous materials could be recycled without any rhodium leaching, being active even in the absence of a solvent. High turnover numbers were obtained in the hydroformylation of either 1-hexene or 1-decene. However, the characteristics of the matrix could not be related to the addition (or not) of a hybrid organic–inorganic co-condensation agent, but appeared to depend on the nature of the rhodium complex.

The development of well-defined catalyst systems that combine good catalytic activity with facile and quantitative catalyst/products separation is still a challenge. An approach to facilitate catalyst recovery is the attachment of homogeneous catalysts to inorganic or hybrid organic–inorganic matrices. Inorganic matrices such as silica are advantageous catalyst supports due to their physical strength and chemical inertness. The entrapment of homogeneous catalysts inside the porous system of silica matrices prepared by the sol–gel method appears to be a promising strategy for catalyst recovery.¹

The addition of hybrid organic–inorganic co-condensation agents $[(RO)_3Si-R'-Si(OR)_3]$ to the classical sol–gel precursors $[Si(OR)_4]$ leads to three-dimensional networks with an organic fragment as an integral component. Such hybrid inorganic–organic matrices have been studied by many groups,^{2–4} with polysiloxane-bound transition metal complexes being extensively studied by Lindner *et al.*⁵ Although the entrapment of hydroformylation catalysts, bearing or not a hydrolysable ligand, inside the porous system of inorganic matrices has been reported,^{6,7} there are no studies concerning the characteristics of the matrix leading to a leach-proof system. In related works we have noticed that, at least in the absence of a hydrolysable ligand [*i.e.*, a ligand bearing an $-Si(OR)_3$ group], in order to avoid leaching the matrix should present a microporous system.⁸ In this work we investigated the effects of the nature of the precursor complex, of the phosphine and also of the presence of a hybrid co-condensation agent on the properties of the matrix as well as on the recycling of the resulting hydroformylation catalysts.

Experimental

Materials

$RhCl_3 \cdot 3H_2O$ (Strem), $[RhCl(COD)]_2$ (Strem), $[Rh(CO)_2(acac)]$ (Strem), tetramethylorthosilicate (TMOS, Aldrich), dichloromethane (Merck), 1-hexene (Aldrich), styrene (Aldrich) and cyclooctane (Fluka) were used as received. Toluene (Merck) and tetrahydrofuran (Merck) were distilled under argon over sodium/benzophenone. $[Rh(OMe)(COD)]_2$, $[RhCl(CO)_2]_2$, $[Rh(acac)(COD)]$ and 1,4-bis(triethoxysilyl)benzene were prepared according to published methods.^{9–12}

Catalyst preparation. In a typical preparation, 0.01 mmol of the rhodium complex and 0.05 mmol of the phosphine were dissolved in 6 ml of THF (degassed through several cool-thaw cycles) in a 50 ml Schlenk flask. After 15 min stirring, 2.0 ml (11.10 mmol) of deionized water, 2.0 ml (13.56 mmol) of TMOS (tetramethylorthosilicate), 1.0 ml (3.39 mmol) of 1,4-bis(triethoxysilyl)benzene (co-condensation agent), 1.0 ml (24.69 mmol) of methanol and 4 drops of a 3% solution of $(AcO)_2Sn(Bu)_2$ in polydimethylsiloxane (Dow Corning) were added to the yellow solution. The inorganic matrices were prepared in the same way, but without the addition of the co-condensation agent. The resulting solution was stirred for 15 min and then allowed to stand for at least overnight until gelation. The gel was then dried under vacuum, washed with CH_2Cl_2 in a Soxhlet and dried again under vacuum. The resulting yellow-orange materials were stored under air at room temperature.

Catalytic experiments

All catalytic experiments were performed in a 100 ml stainless steel Parr reactor. The reaction temperature was kept at 80 °C and the solution was stirred at 300 rpm. In a typical experiment, 2–5 μ mol of the rhodium complex (~ 0.250 g of the catalyst), 0.28 g (2–5 mmol) 1-hexene ($[Rh]/[olefin] \sim 1/1000$); 0.1 g cyclooctane (internal standard) and 30 ml of THF (solvent) were employed. The reactor was first purged with H_2 , and then pressurized at 50 bar ($CO/H_2 = 1/1$). For recycling experiments, the catalyst was separated by filtration, washed in a Soxhlet with CH_2Cl_2 , dried under vacuum and used in a new run. GC analyses were performed in an HP5890 series II gas chromatograph, equipped with an HP5 capillary column (50 m \times 0.2 mm) and a flame ionization detector. Products were quantified using calibration curves obtained with standard solutions.

Catalyst characterization

Nitrogen adsorption isotherms were determined at $-196^\circ C$ with a Micromeritics ASAP 2010 automated porosimeter. All calculations were performed using the associated Micromeritics software. Samples were degassed at 80 °C for a minimum

of 24 h prior to measurements. Sample size varied from 200 to 300 mg.

Rhodium concentrations were determined through ICP-AES analyses (Perkin-Elmer Optima 3000 DV).

Solution ^{31}P NMR spectra were recorded on a Gemini 300 P instrument at 121.5 MHz, in CDCl_3 . ^{31}P CP-MAS NMR analyses were carried out on a Varian INOVA 500 spectrometer, at 202 MHz, using H_3PO_4 as a reference. The contact time was 1 ms with a 4 s delay between each scan. Around 16 000 scans were accumulated. ^{29}Si CP-MAS NMR analyses were performed on the same spectrometer. The contact time was 2 ms with a 1.1 s delay between each scan. Around 8000 scans were accumulated. Double-bearing zirconia rotors were employed.

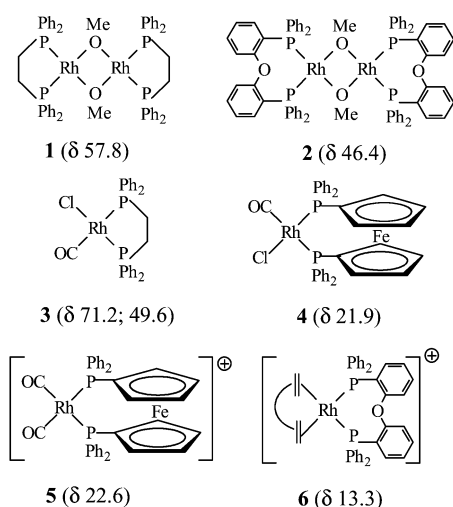
Scanning electron micrographs were obtained using a Jeol-JMS T300 equipment. TEM images were obtained on a Zeiss CEM-902 apparatus equipped with a CCD-Proscan camera and a high speed/slow scan system controller. The samples were suspended in *iso*-propanol and dispersed on carbon-coated copper grids.

Results

In order to determine the effects of the nature of the rhodium complex on the structure of the matrix, four different precursors, *viz.* $[\text{RhCl}(\text{CO})_2]_2$, $[\text{Rh}(\text{OMe})(\text{COD})]_2$, $[\text{Rh}(\text{CO})_2(\text{acac})]$ and $[\text{Rh}(\text{COD})(\text{acac})]$, as well as three chelating phosphine ligands, *viz.* dppe, DPEphos and dppf, characterized by different bite angles (78, 102 and 99°, respectively¹³), were employed. The expected resulting complexes, according to the ^{31}P NMR spectra of the corresponding solutions, are shown in the Scheme. We tried to prepare both inorganic, systems **a**, and hybrid matrices [in this case by using $(\text{EtO})_3\text{Si-Ph-Si}(\text{OEt})_3$ as a co-condensation agent], systems **b**, with each rhodium complex/phosphine pair. However, in the case of $[\text{RhCl}(\text{CO})_2]_2/\text{dppf}$ we failed to prepare the inorganic matrix owing to precipitation of the rhodium complex. All systems were tested in the hydroformylation of 1-hexene and most were also characterized by N_2 adsorption-desorption isotherms. The corresponding results are summarized in Table 1. Some systems were also characterized by ^{31}P and ^{29}Si CP-MAS NMR and/or electron microscopy.

Catalytic experiments

All systems were active in the hydroformylation of 1-hexene but in several cases (systems **1b**, **2a,b**, **5a,b**, and **6a,b**) a high level of Rh leaching was observed (Table 1). System **1a**



Scheme 1 Rhodium species as characterized by ^{31}P NMR.

$([\text{Rh}(\text{OMe})(\text{COD})]_2 + \text{dppe})$ was active in at least 8 runs, the activity increasing in each run. Conversely, the catalytic activity of system **3a** ($[\text{RhCl}(\text{CO})_2]_2 + \text{dppe}$) decreased in each of 5 runs. Except in two cases with high rhodium leaching, isomerization of the substrate, mainly to *trans*-2-hexene, was always observed. The ratio between linear and branched aldehydes varied from 1.6 to 2.6 for the leachless systems (**1a**, **3a**, **3b** and **4b**), the dppe-based catalysts leading to higher *n/i* values. Hybrid matrices based on $[\text{RhCl}(\text{CO})_2]_2 + \text{dppe}$ or dppf (systems **3b** and **4b**, respectively) turned out to be the best catalysts among those studied (higher turnover numbers and hydroformylation/isomerization ratios).

These two systems were also tested in reactions without a solvent. As it can be seen in Table 2, high turnover numbers were obtained in all cases, even when using 1-decene as a substrate (Table 2, 2nd row) without any rhodium leaching. Table 2 also shows that the entrapped catalysts are less active than their homogeneous counterparts, which was indeed expected owing to the diffusion problems intrinsic to a porous material. Nevertheless, for similar conversions, using THF as a solvent the entrapped catalysts were more selective (higher *n/i* values) than their homogeneous counterparts. For comparison, some homogeneous experiments were also carried out without addition of phosphines: these complexes were far less selective than the entrapped catalysts, suggesting that the complexes depicted in the Scheme are indeed the precursors of the active species.

System **3b** was further tested in the hydroformylation of styrene. Using $[\text{Rh}]/[\text{olefin}] = 1/1000$, a turnover number of 770 was observed after 24 h, with *n/i* = 0.5.

Nitrogen adsorption/desorption experiments

The nitrogen adsorption-desorption isotherms of catalysts **1a**, **3b** and **4b** are of type I (IUPAC classification¹⁴), characteristic of microporous systems. In only one case was a small hysteresis in their desorption branches observed (system **3b**, Fig. 1), suggesting that the pores are mainly smooth and cylindrical, with a low contribution of mesopores.¹⁵ The volumes adsorbed at the lowest relative pressure indicate, in all cases, a large volume of extremely small pores. The Horvath-Kawazoe differential pore volume plots for catalysts **1a** (as a fresh sample and after 8 runs) and **3b** are shown in Fig. 2 (catalyst **4b** presented a homogeneous pore distribution). BET surface areas, pore volumes and average pore size determined from the isotherms are presented in Table 1.

Catalysts **2b**, **5a,b** and **6a,b** are characterized by type IV isotherms (Fig. 1), with catalyst **6a** (as well as **5a**) presenting a type H2 hysteresis loop (IUPAC classification¹⁴). The shape of this isotherm indicates the presence of ink-bottle or narrow-mouth shaped pores.¹⁵ The hysteresis loop observed in the isotherm of catalyst **2b** is of type H4, indicating that its mesoporous system is not well defined. The volumes adsorbed at the lowest relative pressure represent *ca.* 50% and 30% of the total pore volume for catalysts **2b** and **6a** (as well as **5a**), respectively, indicating in both cases a significant volume of extremely small pores. Systems **5b** and **6b** present larger pores (up to 12 nm), with the volume adsorbed at the lowest relative pressure representing less than 10% of the total pore volume for these catalysts. The BJH adsorption pore size distributions for some of these systems are shown in Fig. 2. We failed to obtain isotherms for systems **1b** and **3a**.

^{29}Si and ^{31}P CP-MAS NMR

In order to try to correlate the degree of condensation with the porosity of the hybrid or inorganic matrices, some catalysts were also analyzed by ^{29}Si CP-MAS NMR. These catalysts were chosen based both on their different performances in catalysis and on the nature of their porous systems. Fig. 3 shows the spectra obtained for catalysts **2b**, **4b** and **5a**. For the hybrid

Table 1 Composition, physical characteristics and catalytic activity of the inorganic (**a**) and hybrid (**b**) systems.^a

System	Rhodium complex	Rh wt %	Phosphine	BET surface area/m ² g ⁻¹	Pore volume/cm ³ g ⁻¹	Average pore diameter/nm	Run	% Conv ^b	n/i ^c	H/I ^d	TON ^e	Rh leaching ^f
1a	[Rh(OMe)(COD)] ₂	0.25	dppe	480	0.21 ^g	0.70 ^g	1	34	2.6	1.7	340	Colorless solution
							2	32	2.5	1.7	320	
							4	40	2.5	1.6	400	
							5	57	2.5	1.5	570	
							8	65	2.0	1.8	650	
1b	[Rh(OMe)(COD)] ₂	0.15	dppe	420	0.18 ^g	0.72 ^g	1	59	2.6	1.8	590	High
2a	[Rh(OMe)(COD)] ₂	0.24	DPEphos	n.d.	n.d.	n.d.	1	38	2.6	1.1	380	0.7%
2b	[Rh(OMe)(COD)] ₂	0.15	DPEphos	420	0.27 ^h	4.36 ^h	1	55 ⁱ	2.3	1.3	550	20%
3a	[RhCl(CO) ₂] ₂	0.33	dppe				1	65	2.0	2.0	650	Colorless solution
							2	46	2.4	1.7	460	
							3	39	2.4	1.7	390	
							5	10	2.4	1.9	100	
							1	46	2.5	1.7	810 ^k	
3b	[RhCl(CO) ₂] ₂	0.23	dppe	370	0.17 ^g	0.85 ^g	5	67	2.1	1.9	990 ^k	Colorless solution
4b	[RhCl(CO) ₂] ₂	0.21	dppf	410	0.10 ^g	0.66 ^g	1	74	1.6	3.0	740	Colorless solution
							2	70	1.9	2.4	700	
							6	71	1.7	2.6	710	
5a	[Rh(CO) ₂ (acac)]	0.12	dppf	670	0.53 ^h	2.95 ^h	1	27 ^j	2.5	—	270	High
5b	[Rh(CO) ₂ (acac)]	0.07	dppf	390	1.04 ^h	12.1 ^h	1	91	0.8	19.2	910	High
6a	[Rh(COD)(acac)]	0.03	DPEphos	750	0.60 ^h	2.68 ^h	1	51	0.7	4.1	510	High
6b	[Rh(COD)(acac)]	0.02	DPEphos	360	1.00 ^h	12.5 ^h	1	90	0.7	—	900	High

^a Reaction conditions: [Rh]/[1-hexene] ~ 1/1000; 50 bar ([CO]/[H₂] = 1/1; 80 °C; 24 h. ^b Conversion to aldehydes. ^c n/i = ratio between linear and branched aldehydes. ^d H/I = ratio between conversion to hydroformylation and isomerization products. ^e TON = mol of aldehydes per mol of rhodium. ^f Colorless solution: < 0.7% Rh. ^g Horvath–Kawazoe method. ^h BJH method. ⁱ 3 h. ^j 5 h. ^k [Rh]/[1-hexene] ~ 1/1800.

matrices (**2b**, **4b**), signals corresponding to T¹ [–Si(OR)₂R', δ ~ –62], T² [=Si(OR)R', δ ~ –71] and T³ (≡Si–R', δ ~ –79) sites, owing to the presence of the co-condensation agent, were observed. Since all spectra were recorded using exactly the same conditions, the relative intensities of the signals of the Q² [=Si(OH)₂, δ ~ –91], Q³ [=Si–OH, δ ~ –101] and Q⁴ (≡Si–O–Si≡, δ ~ –101) sites, Table 3, can be used to qualitatively compare the relative degree of TMOS condensation between hybrid and inorganic matrices. Higher Q⁴/Q³ and Q⁴/Q² values were obtained with hybrid matrices (Table 3), showing that the condensation degree of TMOS is higher when the co-condensation agent is present. (The absolute degree of condensation cannot be directly determined since the spectra were collected using the cross-polarization technique.) In the hybrid matrices, the relative degree of condensation of 1,4-bis-(triethoxysilyl)benzene, which is based on the T³/T² ratios, does not seem to be related to the porosity of the matrix: T³/T² ratios for a mesoporous and a microporous matrices do not vary significantly (Table 3).

Samples **1a**, **2b**, **3a**, **4b** and **5a** were also analyzed by ³¹P CP-MAS NMR. Nevertheless, except for the system **3a**, which was analyzed as a fresh sample and also after the catalytic experiments (*i.e.*, after 5 runs, see Fig. 4), the spectra obtained

for all systems showed only resonances ascribed to the free ligand and/or to the corresponding phosphine oxide. Owing to the low rhodium concentration in all cases, and also to the excess of phosphine employed, the nonobservation of a signal ascribed to a rhodium-coordinated phosphine does not imply that such a species was not formed.

Electron microscopy

Fig. 5 shows transmission electron micrographs obtained from microporous, **3b** (top left), and mesoporous, **5a** (top right), materials. The TEM image from system **3a** (bottom, left) suggests a very dense matrix. The corresponding SEM image (bottom, right) shows holes with diameters varying from 0.4 to 1.3 μm. Taking into account that this material was able to entrap a relatively large amount of rhodium and did not present any leaching in the catalytic experiments, these micrographs suggest a nonporous structure with packed microporous domains. TEM experiments also showed that clustered rhodium particles were not formed in the cases studied.

Discussion

The co-condensation agent was expected to reduce the degree of 3D-cross-linking, decreasing the rigidity and improving the swelling properties of the resulting matrix. It was also expected to affect the porous system and thus the diffusion of the reagents inside the matrix.

Comparison of the systems **1a** and **1b** with **3a** and **3b** shows that there is no clear correlation between the presence of the co-condensation agent and the catalytic performance: when the precursor is [RhCl(CO)₂]₂ (systems **3a** and **3b**), the hybrid catalyst shows no leaching and keeps its catalytic activity for at least 5 runs. If the precursor is [Rh(OMe)(COD)]₂ (systems **1a** and **1b**), the presence of the co-condensation agent leads to a high rhodium leaching and catalysis seems to take place in solution. On the other hand, in the absence of the co-condensation agent (system **1a**), the catalytic activity increases in each run, suggesting that the formation of the active species (a rhodium hydride) is rather slow, its concentration increasing in

Table 2 Catalytic performance of some hybrid systems without solvent as compared to homogeneous systems in THF.^a

System	% Conv. ^b	n/i	H/I	TON ^c
3b [RhCl(CO) ₂] ₂ + dppe	35	1.7	11.9	1750
3b [RhCl(CO) ₂] ₂ + dppe	72	1.4	2.9	3600 ^d
4b [RhCl(CO) ₂] ₂ + dppf	42	2.2	9.2	2300
	64	2.4	21.3	3180 ^e
[Rh(OMe)(COD)] ₂ + dppe	56	1.7	1.9	2800 ^f
	67	1.5	2.5	3350 ^g
[RhCl(CO) ₂] ₂ + dppe	34	2.1	1.3	1700 ^g
[Rh(OMe)(COD)] ₂	46	0.80	0.96	2300 ^g
[RhCl(CO) ₂] ₂	46	0.67	0.88	2300 ^g

^a [Rh]/[1-hexene] = 1/5000; 24 h. ^b Conversion to aldehydes. ^c mol of aldehydes per mol of Rh. ^d [Rh]/[1-decene] = 1/5000. ^e 48 h. ^f In THF. ^g 2.5 h. ^h 4 h.

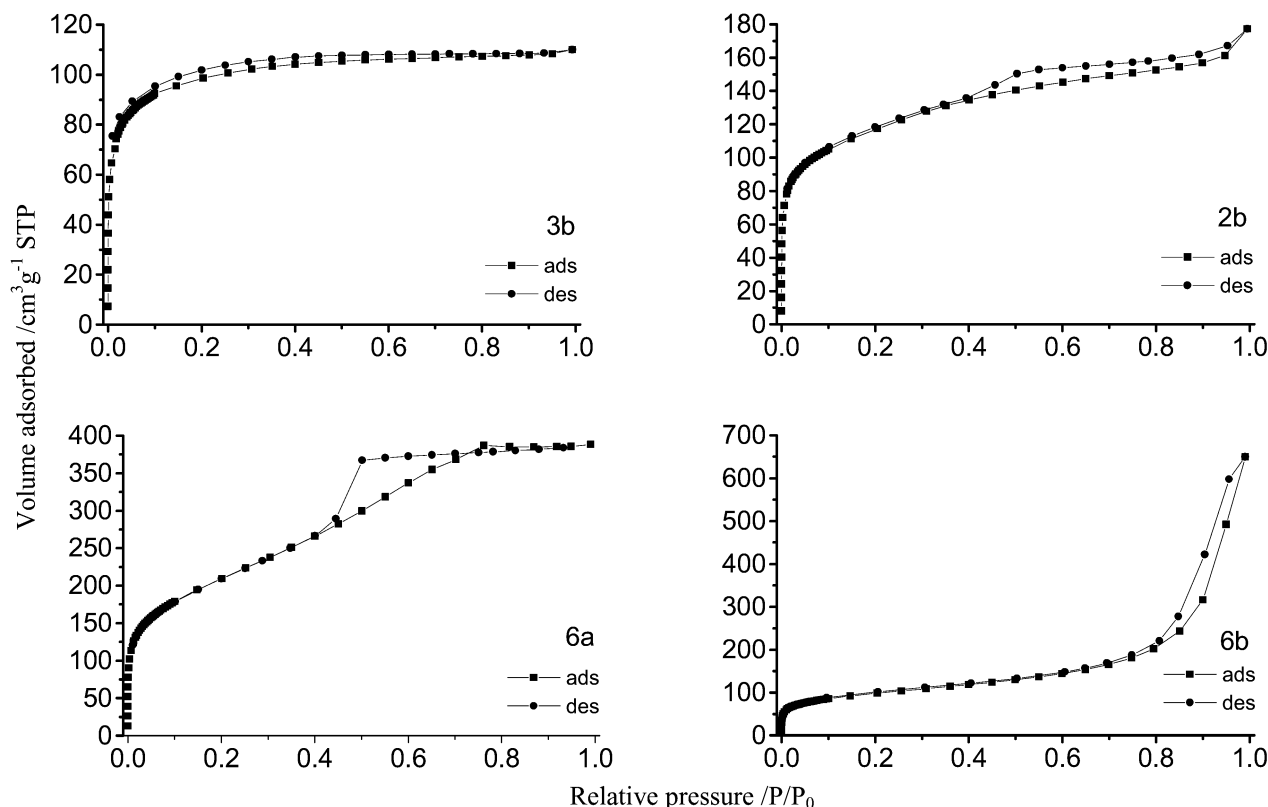


Fig. 1 Nitrogen adsorption/desorption isotherms for several catalysts.

each run. Considering only systems **1** and **3**, it can also be seen that the best catalysts, **1a** and **3b** (without and with co-condensation agent, respectively), are characterized by a microporous system, with a low mesoporous contribution.

The continuous deactivation of system **3a** could be due to degradation of the rhodium complex since metal leaching was not detected; a color change, from yellow to orange, was indeed observed after the first run. Nevertheless, ^{31}P CP-MAS NMR spectra of a fresh sample of system **3a** and after 5 runs show only one broad signal at $\delta \sim 38$, tentatively ascribed to $[\text{RhCl}(\text{dppe})_2]_2$ (δ 35) and/or to the corresponding dppe-oxide (δ 33). Thus, the catalyst deactivation is probably due to pore blockage, as suggested by the dense structure revealed by the transmission electron image.

Comparing the systems **1** through **4**, it can also be seen that the amount of rhodium complex entrapped inside the porous

system is significantly higher in the absence of the co-condensation agent. The higher degree of TMOS condensation obtained by addition of the co-condensation agent could account for this observation: when microporous matrices were obtained (catalysts **1a**, **3b** and **4b**), the hybrid systems showed smaller BET surface areas and pore volumes than the inorganic ones. On the other hand, the relative degree of condensation of the co-condensation agent seems to depend on the nature of the entrapped rhodium complex and cannot be directly correlated to the porosity of the matrix.

Systems **1** to **4** were prepared using $(\text{AcO})_2\text{SnBu}_2$ as a condensation catalyst, allowing gelation to take place overnight. In the other cases it was not employed and gelation took at least 3 days. Systems **5** and **6** were prepared without the tin catalyst since it was expected that cationic rhodium complexes would be able to catalyze the condensation reaction. Rhodium

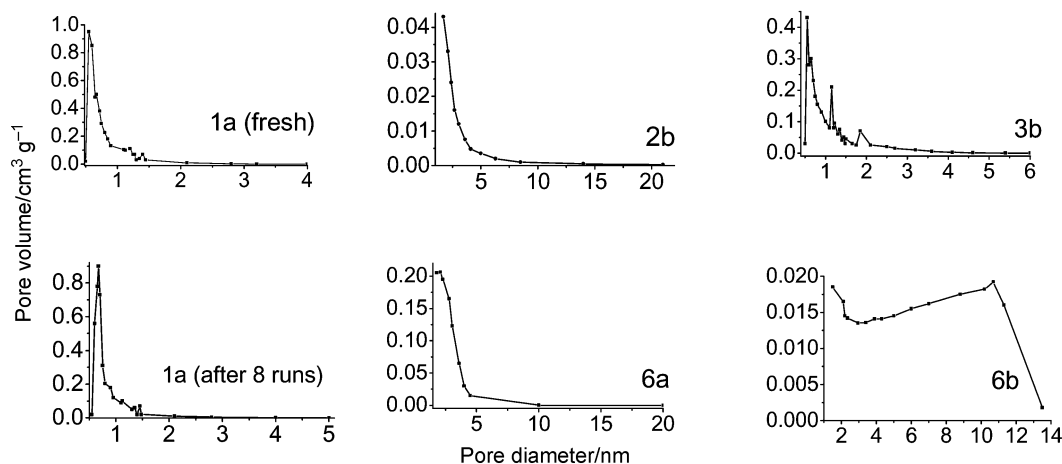


Fig. 2 Pore size distribution for several catalysts.

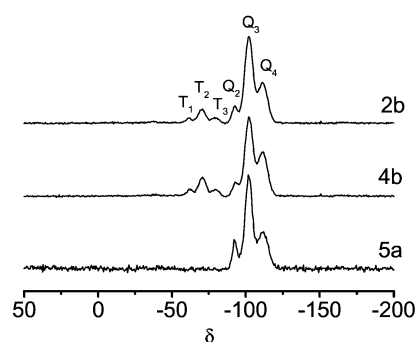


Fig. 3 ^{29}Si CP-MAS NMR spectra for catalysts **2b**, **4b** and **5a**.

Table 3 Relative intensities of ^{29}Si CP NMR signals for some catalysts

Catalyst	Q^4/Q^2	Q^4/Q^3	T^3/T^2	Porous system
5a	1.39	0.43		Mesoporous
1a	1.77	0.36		Microporous
2b	2.46	0.48	0.40	Mesoporous
1b	2.63	0.52	0.50	
4b	3.15	0.58	0.36	Microporous

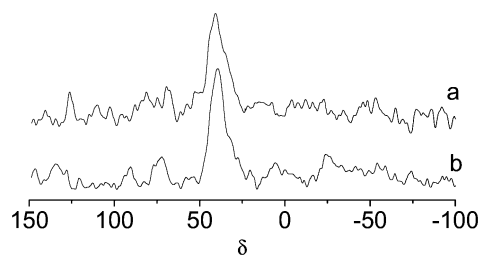


Fig. 4 ^{31}P CP-MAS NMR spectra for **3a**: (a) fresh sample; (b) after 5 runs.

complexes containing the acac^- ligand react with biphosphines leading to cationic species of the type $[\text{RhL}_2(\text{biphosphine})]^+[\text{acac}]^-$ (L = neutral ligand).⁷ The data in Table 1 show that this strategy has led to the entrapment of still lower amounts of rhodium. It can also be observed that when the acac -containing precursors were employed the resulting matrices presented a mesoporous system, which does not seem to be able to entrap adequately the rhodium complexes. Moreover, for systems **5** and **6** the influence of the co-condensation agent was clear: it led to a significant decrease in the volume of micropores and to a large distribution of mesopores. Therefore, the rhodium complexes were washed away during

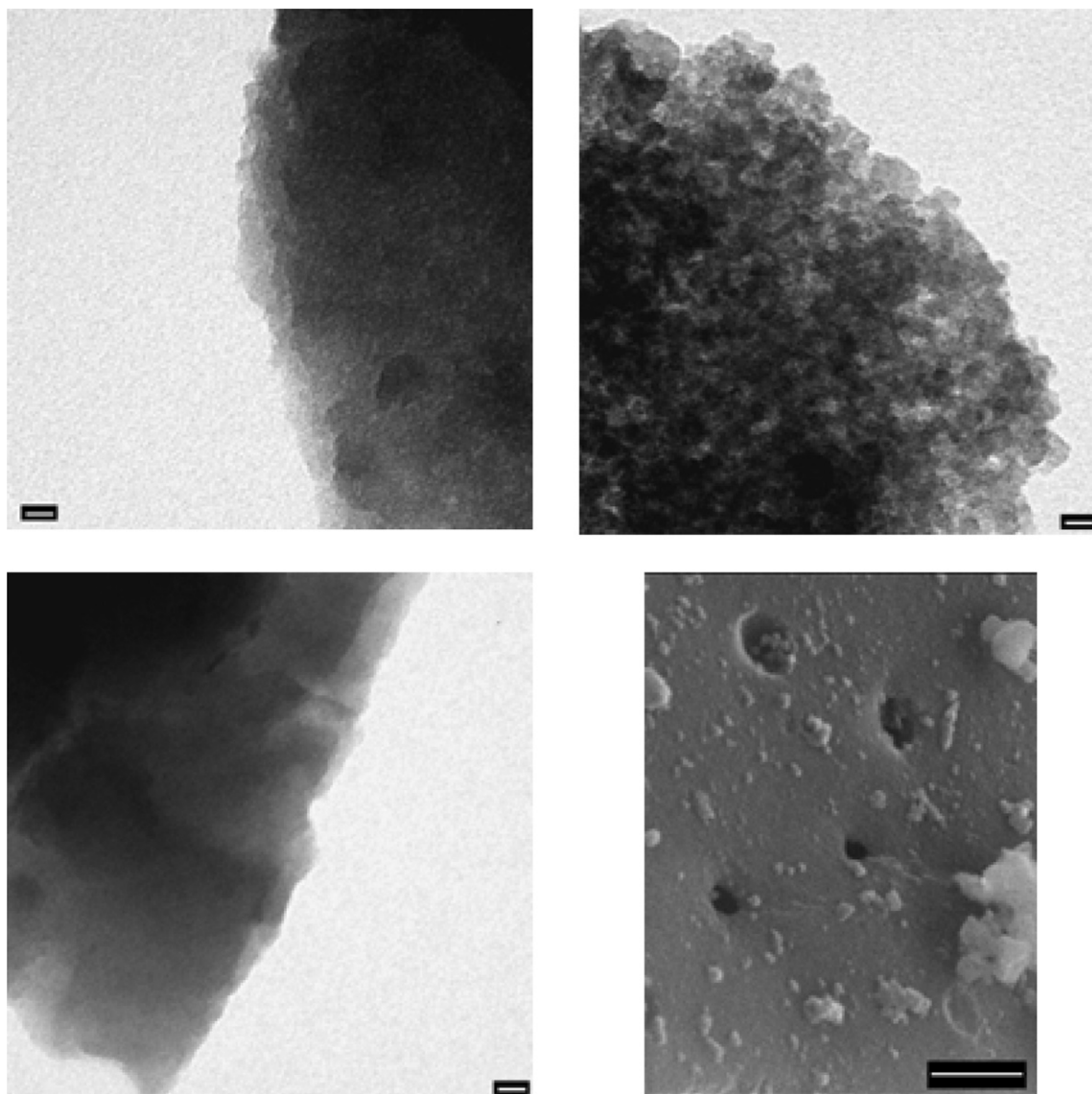


Fig. 5 TEM images (bar: 10 nm) from systems **3b** (top left), **5a** (top right), **3a** (bottom left); SEM image from system **3a** (bottom right; bar: 2 μm).

the Soxhlet washing, and the very small amount (~ 0.02 wt %) of remaining complexes leached in the catalytic experiments.

All systems prepared with DPEphos, starting either with $[\text{Rh}(\text{OMe})(\text{COD})]_2$ or $[\text{Rh}(\text{COD})(\text{acac})]$, showed a high rhodium leaching and also a mesoporous system (for the three analyzed cases). The higher bite angle of this ligand along with its large flexibility ($86\text{--}120^\circ$)¹³ might favor larger pores in order to better accommodate a more voluminous complex.

From all data available, it appears that a microporous system is necessary to avoid leaching. This conclusion is in agreement with results reported in the case of entrapped rhenium or molybdenum epoxidation catalysts, at least when no hydrolysable ligand was employed.⁸ However, the ambiguous results obtained in this work concerning the effects of the co-condensation agent are in contrast with previous works: for rhenium and molybdenum epoxidation and ruthenium hydrogenation catalysts, at least with the same TMOS (or TEOS)/1,4-bis-(triethoxysilyl)benzene molar ratio (4/1), the co-condensation agent ensured a microporous system and higher surface areas.^{8,16}

Conclusions

Rhodium complexes derived from $[\text{RhCl}(\text{CO})_2]_2$ or $[\text{Rh}(\text{OMe})(\text{COD})]_2$ and dppe or dppf could be prepared *in situ* and entrapped inside the porous systems of inorganic or hybrid matrices *via* the sol–gel method. Only the microporous systems could be re-used without rhodium leaching. The hybrid systems **3b** and **4b** turned out to be the best catalysts studied in this work, being highly active and stable for at least 7 days. They are prepared from commercially available phosphines and easily synthesized rhodium precursors. Higher olefins such as 1-decene and styrene could also be hydroformylated. High turnover numbers were obtained in the absence of a solvent. The selectivity to linear aldehydes was, in some cases, higher than that observed in homogeneous solution.

Although the hybrid matrices led to the best catalysts, the presence of the hybrid co-condensation agent did not ensure the formation of a microporous matrix. Its presence seemed to increase the degree of condensation of TMOS. The porosity of the matrix, however, appeared to be more dependent on the

nature of the final rhodium complexes. Thus, it seems that cationic rhodium species favor the formation of mesoporous structures; therefore, acac-containing precursors are to be avoided when no hydrolysable ligand is employed.

Acknowledgements

Financial support from FAPESP, as well as a fellowship to J.D.R.C., are gratefully acknowledged.

References

- 1 J. Blum, D. Avnir and H. Schumann, *Chemtech*, 1999, **29**(Feb.), 32.
- 2 U. Schubert, *New J. Chem.*, 1994, **18**, 1049.
- 3 K. J. Shea and D. A. Loy, *Acc. Chem. Res.*, 2001, **34**, 707.
- 4 (a) R. J. P. Corriu and D. Leclercq, *Angew. Chem., Int. Ed Engl.*, 1996, **35**, 1420; (b) P. Chevalier, R. J. P. Corriu, P. Delord, J. J. E. Moreau and M. W. Chi Man, *New J. Chem.*, 1998, **22**, 423.
- 5 E. Lindner, T. Schneller, F. Auer and H. A. Mayer, *Angew. Chem., Int. Ed.*, 1999, **38**, 2154.
- 6 (a) S. Wieland and P. Panster, *Catal. Org. React.*, 1994, **62**, 383; (b) J. Blum, A. Rosenfeld, N. Polak, O. Israelson, H. Schumann and D. Avnir, *J. Mol. Catal.*, 1996, **107**, 217.
- 7 A. J. Sandee, L. A. van der Veen, J. N. H. Reek, P. C. J. Kamer, M. Lutz, A. L. Spek and P. W. N. M. van Leeuwen, *Angew. Chem., Int. Ed.*, 1999, **38**, 3231.
- 8 (a) K. Dallmann and R. Buffon, *Catal. Commun.*, 2000, **1**, 9; (b) S. Teixeira, K. Dallmann, U. Schuchardt and R. Buffon, *J. Mol. Catal. A: Chem.*, 2002, **182–183**, 167.
- 9 R. Usón, L. A. Oro and J. Cabeza, *Inorg. Synth.*, 1985, **23**, 126.
- 10 J. A. McCleverty and G. Wilkinson, *Inorg. Synth.*, 1966, **8**, 211.
- 11 R. Cramer, *J. Am. Chem. Soc.*, 1964, **86**, 217.
- 12 D. A. Loy, G. M. Jamison, B. M. Baugher, S. A. Myers, R. A. Assink and K. J. Shea, *Chem. Mater.*, 1996, **8**, 656.
- 13 P. C. J. Kamer, J. N. H. Reek and P. W. N. M. van Leeuwen, *Chemtech*, 1998, **28**(Sept.), 27.
- 14 K. S. W. Sing, D. H. Everett, R. A. Haul, L. Moscou, R. A. Pierotti, J. Rouquerol and T. Siemieniowska, *Pure Appl. Chem.*, 1985, **57**, 603.
- 15 C. J. Brinker and G. W. Scherer, *Sol–Gel Science: The Physics and Chemistry of Sol–Gel Processing*, Academic Press, San Diego, 1990, pp. 522–525.
- 16 K. Dallmann and R. Buffon, *J. Mol. Catal. A: Chem.*, 2002, **185**, 187.